respond to discrete energy losses suffered by photoelectrons exciting interband transitions. Alternatively, the structure at $E^*=-11.0$ eV may be ascribed to energy losses suffered by the photoelectrons involving the excitation of both a 7-eV collective oscillation and a 3.5-eV interband transition.

Above an incident photon energy of 9 eV, electron-electron collisions may result in an increased total yield. In particular, for incident photon energies above 12 eV, the photoelectron excitation of 7-eV collective oscillations may give rise to an increased photoelectric yield, since the plasmon decay may result in a single-electron excitation.[25] For incident photon energies above 16 eV the yield may be further increased by the photoelectron excitation of the 11-eV transition. Such processes may explain the monotonic increase in photoelectric yield with increasing energy (Fig. 5) and are consistent with the predictions of very short electron-electron scattering lengths for these energies.[1]

ACKNOWLEDGMENT

The authors would like to thank T. A. Callcott for a critical reading of the manuscript.

[25] W. Steinmann and M. Skibowski, Phys. Rev. Letters **16**, 989 (1966).

PHYSICAL REVIEW B VOLUME 1, NUMBER 2 15 JANUARY 1970

Slow-Electron Mean Free Paths in Aluminum, Silver, and Gold†

H. KANTER
The Aerospace Corporation, El Segundo, California
(Received 4 September 1969)

Beam-attenuation measurements were made on free-standing polycrystalline films of various thicknesses at energies between the work function and several electron volts above. The electron-electron collision mean free paths l_e were determined by correction of the attenuation lengths for electron-phonon scattering lengths l_p deduced from the attenuation temperature dependence. Imperfection mean free paths were negligible. The following results were obtained: for aluminum, $l_e\sim50$ Å and $l_p\sim250$ Å near 5 eV above the Fermi level; for gold, 45 Å$>l_e>$15 Å for energies between 5.5 and 10 eV; and for silver, 42 Å$>l_e>$20 Å for energies between 5.5 and 8 eV. In the energy range between 5.5 and 7.5 eV, it was found that $l_p\sim250$ Å for gold and $l_p\sim400$ Å for silver. All measured l_p were only about two-thirds of the value near the Fermi level. Quinn's theory for l_e in a dense free-electron gas predicts that for aluminum $l_e\sim60$ Å at 5 eV. Exchange corrections in Kleinman's dielectric screening function tend to bring the value closer to the observed one. In silver and gold, considerable interaction of the beam electrons with the d band occurred for which no theory is available as yet. The resulting data were compared with the energy dependence of l_e deduced semiempirically by Krolikowski and Spicer from the density of states obtained from photoemission experiments. Reasonable agreement with presently available data was observed.

I. INTRODUCTION

HOT-ELECTRON mean free paths (MFP) in metals for energies from several tenths of a volt to a few volts above the Fermi level have in the past primarily been measured with photoemission or tunnel-emission techniques. The former method[1] utilizes photoexcited electrons escaping from a metal film into an adjacent semiconductor or into a vacuum. Total yield is measured as a function of film thickness. The electron-attenuation length may be deduced from the data if the optical absorption in the metal film is known. Since this quantity depends critically on film quality and thickness, it must generally be determined separately. Furthermore, the energy is determined by the barrier height at the metal boundary. Variation of energy, thus, requires the use of different substrate materials with possible effects on the film structure. Hence, photoemission techniques are rather complex, and interpretation of the data is prone to error.

The tunnel-emission technique[2] produces hot electrons by field emission from a base metal, through a thin oxide layer, into a metal film deposited on top of the oxide. Variation of the number of electrons escaping through the top layer is measured as a function of thickness. Although in this geometry the electron source is confined to one boundary, the electron energy upon entering the metal film is not well defined because of considerable inelastic scattering in the oxide. Inelastic scattering may be avoided by tunneling through the forbidden gap of the oxide; this, however, restricts the applied potential. Measurement and interpretation of attenuation measurements as a function of energy is, thus, rendered difficult.

For a review of MFP measurements employing these older techniques, the reader is referred to a recent

† Work supported by the U. S. Air Force under Contract No. F04701-69-C-0066.

[1] C. R. Crowell, W. G. Spitzer, L. E. Howarth, and E. E. Labate, Phys. Rev. **137**, 2006 (1962); S. M. Sze, J. L. Moll, and T. Sugano, Solid-State Electron. **7**, 509 (1964).

[2] C. A. Mead, Phys. Rev. Letters **8**, 56 (1962); **9**, 46 (1962); H. Kanter, J. Appl. Phys. **34**, 3629 (1963).

article by Crowell and Sze,[3] which contains all pertinent references.

More recently, MFP determination from photoemission experiments have been refined by evaluation of the energy distributions of photoelectrons as opposed to evaluation of total-yield measurements only. Krolikowski and Spicer[4] calculated the energy dependence of the MFP from density-of-state distributions that were deduced from photoelectron energy-distribution measurements. They then fitted the magnitude of MFP's to give agreement with absolute yield at a certain photon energy. In another method, Eastman[5] utilized the thickness dependence of photoelectron-energy distribution and yield curves for the determination of MFP as a function of energy. While the complexity of the evaluation of the photoemission process has, thus, further increased as compared with simple yield measurements, the methods are applicable to a large number of materials and might turn out to be the primary source of experimental MFP information in the small-energy range. However, for confidence in the validity of this approach, it appears desirable to provide MFP results by an independent and more direct method.

In this paper, we determine MFP by measuring the attenuation of a collimated beam of slow electrons as a function of thickness of free-standing metal films. Since it is assumed that any scattering event removes an electron from the beam, the transport process is very simple, and the MFP is determined rather unambiguously. Variation over a range of energies is possible on a single sample; pinholes and other nonuniformities of the film are easily detected during the experiment; the sample structure is readily observable in an electron microscope. A more rigorous study of the influence of these parameters on attenuation as compared with previously employed methods is, thus, possible. Of course, this technique is restricted to energies in excess of the work function of the metal and, therefore, are larger than 4–5 eV unless barrier-lowering surface layers are used. At these energies, the dominating interactions are electron-electron collisions in the film. Other processes, such as electron-phonon and electron-imperfection interaction, that primarily determine the conduction properties are of only minor importance. Therefore, data obtained by this method do not require major corrections to determine the actual electron-electron interaction MFP and can be readily compared with theoretical predictions for this process.

The experimental setup (Sec. II) and the film preparation and properties (Sec. III) are discussed. Gold (Au) and silver (Ag) were used primarily because these materials are experimentally most readily amenable. Data for aluminum (Al) were taken because the properties of the electronic structure of this material approach those of the dense free-electron gas, and comparison with theoretical MFP calculations based on this model appear justified. During the course of the work, it became apparent that for all materials the state of annealing, exemplified by the crystallite size, has a profound effect on attenuation. Measurements, therefore, were not taken until the attenuation stabilized after repeated temperature cycling between 130 and 420°K, resulting in crystallite sizes that in the film plane exceeded the average film thickness. After a short discussion of the transport process in Sec. IV, attenuation lengths are presented in Sec. V. The temperature dependence of attenuation remaining after completion of the annealing process could be interpreted as being caused by electron-phonon interaction. The associated MFP was applied as a relatively small correction to the measured attenuation lengths in order to obtain the electron-electron interaction MFP's. Further corrections appeared to be unnecessary, since conductivity measurements on the films indicated the residual imperfection MFP to be negligible at the energy values considered here.

In Sec. VI, the measured electron-electron collision lengths of 50 Å for Al at 5 eV above the Fermi level are compared with the theoretical prediction[6] of about 60 Å based on the dense free-electron gas model. Exchange corrections based on the improved dielectric screening functions of Kleinman[7] tend to remove the discrepancy. We compared our result for Al with recent attenuation measurements in thin-film triode structures near 2.5 eV above the Fermi level and found reasonable agreement.[8]

Since the d-band edge in Au and Ag is positioned about 2 and 4 eV, respectively, below the Fermi level, interaction of the beam electrons in these materials with d electrons can occur. No theory for this process is available as yet. The energy dependence of our measured electron-electron interaction MFP for Au and Ag is, therefore, compared with semiempirical MFP curves calculated by Krolikowski and Spicer on the basis of density-of-state distributions obtained from photoelectron energy measurements.[4] These curves represent the energy dependence of our MFP's reasonably well and, furthermore, relate our data quite satisfactorily with those published by Sze *et al.*[9] for energies near 1 eV. In general, the data tend to support the applicability of the one-electron model for the electron-electron interaction process as a good approxi-

[3] C. R. Crowell and S. M. Sze, *Physics of Thin Films* (Academic Press Inc., New York, 1967), Vol. 4, p. 325.

[4] W. F. Krolikowski, Stanford Electronics Laboratory Technical Report No. 5118-1, Stanford University, 1967 (unpublished); W. F. Krolikowski and W. E. Spicer, Phys. Rev. **185**, 882 (1969); this issue, B **1**, 478 (1970).

[5] D. E. Eastman, Solid State Commun. **8**, 41 (1970); and (private communication).

[6] J. J. Quinn, Phys. Rev. **126**, 1453 (1962).

[7] L. Kleinman, Phys. Rev. **172**, 383 (1968).

[8] E. E. Huber, F. L. Johnston, and C. T. Kirk, Jr., J. Appl. Phys. **39**, 5104 (1968).

[9] S. M. Sze, C. R. Crowell, G. P. Carey, and E. E. Labate, J. Appl. Phys. **37**, 2690 (1966).

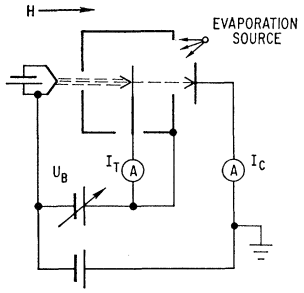

FIG. 1. Schematic of apparatus. The beam is collimated by a 200-Oe magnetic field. The beam diameter is about 1 mm; the target diameter, 2 mm. With the help of deflection plates, the beam could be moved across the film surface so that the detection of pin holes and other film nonuniformities was greatly facilitated. The normal component of the beam energy spread as measured at the collector without a target inserted was 0.5 eV between the 10 and 90% points of the collector-current–versus–retardation-voltage curve. (Surface potential variations at the collector are, thus, included in the energy spread value.) Typical bombarding currents were 2×10^{-7} A (thereby, the nearly 60% open area of the film support screen is considered). Currents leaving the film were in the 10^{-11}–10^{-14} A region and were measured with a vibrating Reed electrometer. The noise current was about 10^{-14} A.

mation. Section VI concludes with a comparison of our measured electron-phonon MFP's, valid near 6 eV above the Fermi level, with those deduced from conductivity measurements, applicable at the Fermi energy level. We find that for all three investigated metals the electron-phonon MFP near 6 eV is only about two-thirds of that near the Fermi level. No quantitative theoretical explanation of this fact is available at present.[10]

II. EXPERIMENTAL

The experimental setup is sketched in Fig. 1 and its potential diagram in Fig. 2. A simple diode gun struc-

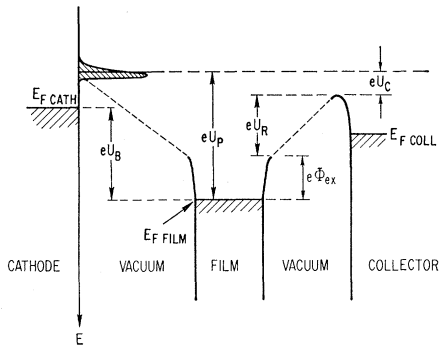

FIG. 2. Energy diagram of apparatus. The beam energy was determined as follows: Beam retardation at the collector allowed us to determine the potential difference between collector surface and average beam energy; any desired U_C, thus, could be set. The break-off point of the curve labeled I_c (retarded) in Fig. 3 occurs for $U_R\equiv0$, i.e., collector and exit-film potential are at the same level; hence, U_R can be read off the abscissa of Fig. 3. The work function for freshly evaporated material is published. We used 5.2 eV for Au and 4.5 eV for Ag.

[10] H. Kanter, Appl. Phys. Letters **10**, 73 (1967). A comparison of MFP values for Au with those of previous investigators is given.

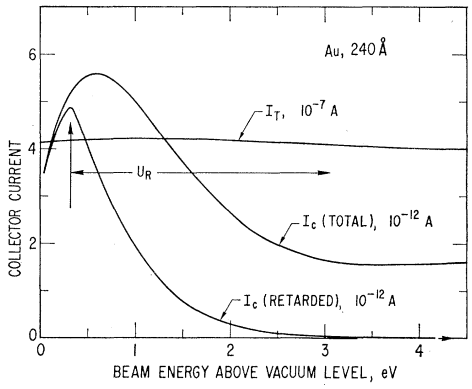

FIG. 3. Typical recorder plot of collector current versus beam energy at constant film thickness. I_c (total) depicts the collector current comprised of all electrons leaving the film regardless of energy. I_c (retarded) records only electrons whose normal energy component has decreased by less than about 0.5 eV.

ture produces an electron beam that, after acceleration to an energy between zero and several electron volts, enters an electric field free space with a target at the center. The target consists of a thin polycrystalline metal film, 150–400 Å thick, supported by an electron-microscope specimen screen. Electrons leaving the target region are collected with an Aquadag-covered plate to which a retarding potential can be applied. The complete structure is immersed in a collimating magnetic field of 200 Oe. The target-holder temperature is variable between −160 and +200°C. Material can be deposited onto the target film *in situ*, the amount being monitored with a crystal-oscillator balance.

During a typical run with Au or Ag films, the collector current was measured as a function of beam energy at constant beam current; the resulting plots are shown in Fig. 3. The curve labeled I_c (total) represents all electrons leaving the film, regardless of energy. The initial rapid increase reflects the rise of the electron energy above the exit-surface potential of the film. At larger energies, however, strong attenuation causes the curve to bend down until, near 4 eV, it reaches a minimum. As indicated by measurements of the normal average energy of the collected electrons (not shown), most electrons up to about 1.5–2 eV above the film-exit potential lost little energy, while at higher energies slower electrons with energy close to the exit barrier began to escape from the film. These electrons were dominant beyond the minimum in the curve, and their number slowly and monotonically increased with further increases in energy.

With the collector potential fixed at about 0.5 eV with respect to mean beam energy (U_C in Fig. 2), the curve labeled I_c (retarded) of Fig. 3 followed. The collector current then dropped rapidly with an increase in beam energy when the collector potential exceeded the film-exit potential, and all electrons with excessive energy loss in the normal direction were rejected. The loss might have been caused by either actual energy

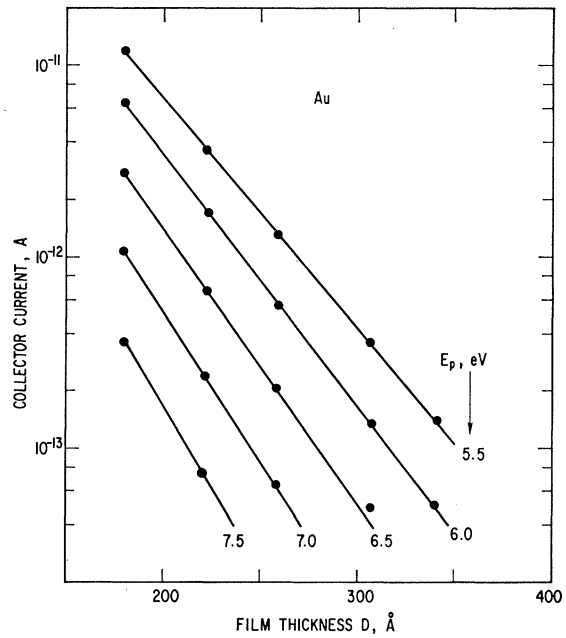

FIG. 4. Typical collector-current–versus–thickness curves for Au at various electron energies obtained by *in situ* evaporation. The support film is 180 Å thick. The independence of slope on thickness together with the clearly observable change of the slopes with energy is taken as evidence that the deposited layers were continuous. Extrapolation of the line for $E_P = 5.5$ eV to zero thickness gives a collector current of $I_c(D \to 0) \approx 10^{-9}$ A, i.e., a factor of near 0.02 below the primary current.

loss or by momentum deflection. The collector selects only electrons whose energy and momentum have not been changed appreciably by passing through the film.

Curves of the type labeled I_c (retarded) in Fig. 3 for Au and Ag were taken at various thicknesses, increased by *in situ* vapor deposition. The data were converted to semilog plots of collector current versus thickness, with the beam energy as a parameter[11] (Fig. 4). From the slope of the lines, attenuation lengths for energies between about 5.5 and 7.0 eV above the Fermi level were obtained. (All subsequently quoted energy values are measured from the Fermi level of the film.) For larger energies, 7–11 eV, only relative measurements were made. On the thinnest possible Au and Ag films, the energy dependence of the attenuation lengths was deduced from the observed energy dependence of the beam transmission. Since we measured with a fixed potential between collector and cathode, the collector potential varied with respect to the film surface and required corrections for equivalent collector efficiency. The corrections were made on the assumption of a cosine distribution of angle of the emerging electrons, commensurate with the observed difference between total and retarded collector currents at energies below 7 eV (Fig. 3). We used the resulting relative attenuation lengths to extend the absolute attenuation lengths to nearly 10 eV.[12] The complete energy dependence of attenuation in Au and Ag is displayed in Fig. 5. The agreement in the overlap region near 7 eV of the slope of the curves obtained by both the absolute and the relative method is excellent.

The data for Al were taken by a different approach since the *in situ* deposition technique could not be used (Sec. III). Films of various thicknesses were inserted into the beam apparatus, and collector currents were measured. The oxide layer on the exit-film surface prevented the use of the retarding technique, since electrons could only be collected at potentials positive with respect to the Al work function. Apparently, a field had to be established across the oxide. At collector potentials of more than 1 eV above the Al work function, the collector current was independent of potential and reproducible. Measurements made under this condition resulted in curves of the type labeled I_c (total) in Fig. 3. Since retardation in this case is provided by the exit barrier (work function) of the Al film, definition of energy of the collected electrons is lost at beam energies much in excess of the work-function value.

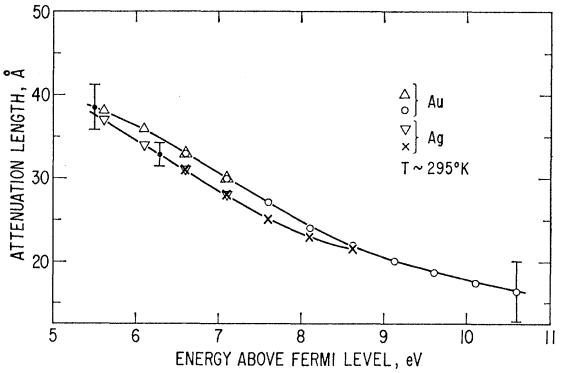

FIG. 5. Measured attenuation length for polycrystalline Au and Ag films. The triangular points were obtained from collector-current–versus–thickness curves (Fig. 4). The crossed and circular points were obtained from collector-current–versus–beam-energy curves (Fig. 3). The latter data were matched with the former. The error bars at the left-hand side represent scatter of the slopes of the collector-current–versus–thickness curves. The error bar at the right-hand side of the curve for Au includes the uncertainty of the effective thickness of the films. The thinnest films that could be made (170 Å) had to be "annealed" for long periods so that they would be sufficiently transparent for 10-eV electrons.

[11] Beam energy refers to the average normal-energy component. The beam spread was 0.5 eV. The collector accepts electrons with a normal-energy component of not less than the average beam energy minus 0.5 eV. The energy window at the collector is limited at the low-energy side by the size of the cone of acceptance and at the high-energy side by the rapid increase in attenuation with energy. The "half-width" of the effective energy window, thus, extends from about 0.3 eV below average beam energy to 0.2 eV above.

[12] Collector current was not measurable for beam energies larger than 10 eV ($I_c < 10^{-14}$A). With the collector potential adjusted in such a manner that the cone of acceptance was constant with energy and permitted collection for a maximum energy loss of 10% of the primary energy, collector current at larger beam energies could only be observed when in excess of 4 keV for Au and Ag and 1 keV for Al. For the latter material, characteristic energy losses were observed, permitting the determination of the scattering cross section. [H. Kanter, Phys. Rev. B 1 (to be published)].

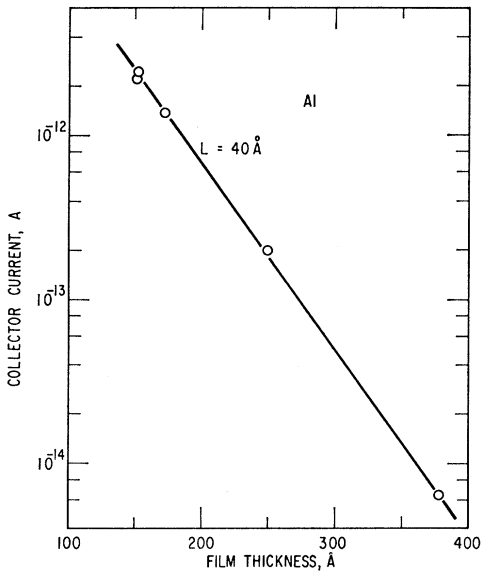

FIG. 6. Collector-current–versus–thickness relation for Al films. These films were prepared in a system separate from the beam apparatus. The collector potential had to be nearly 1 V positive with respect to the film surface in order to reach saturation of current through the oxide.

Therefore, the data were converted to current-versus-thickness plots at 5-eV beam energy only (Fig. 6), which should be representative for electrons within the 4.5–5.5-eV region; the attenuation length was 40 Å. The minimal scatter of points (Fig. 6) indicates that the influence of the strongly attenuating oxide layers may be considered independent of film thickness.

III. FILM PREPARATION

Metal films 150–400 Å thick were vapor-deposited on nitrocellulose films supported by electron-microscope specimen screens. The substrate films were subsequently dissolved in amyl acetate. The deposition conditions were as follows: Source purity for Au and Ag was better than 99.999% and for Al was 99.998%; deposition rate was 2–5 Å/sec; background pressure was 2×10^{-10} to 2×10^{-9} Torr, depending on bake temperature and duration; maximum pressure during evaporation for Al was between 10^{-9} and 5×10^{-8} Torr and for Au and Ag was between 5×10^{-9} and 2×10^{-7} Torr; substrate temperature was 40°C or higher for Au and Al and was near −50°C for Ag. The film thickness was monitored with a crystal-oscillator balance, whose calibration agreed within a few percent with the manufacturer's specification.[13] Quoted thicknessse are, thus, mean values obtained by using bulk densities.[14]

The yield of pinhole-free films prepared under these conditions was excellent for Au and fair for Al. The method was successful only for a few Ag films with the substrate at the lower temperature. The presence of pinholes [Fig. 7(b)] became apparent in the beam apparatus from nonzero collector currents at beam energies in excess of 5 eV, where retarded collector currents are normally below the noise level (Fig. 3). Annealing by heating the films (of either material) did not appear to open up pinholes on a microscopic scale; this could lead to eventual rupture only when heated beyond 180°C. The structure of typical annealed films of all three materials, together with their diffraction patterns, are shown in Fig. 7. Note that the crystallite size in the film plane considerably exceeds the film thickness, particularly for Au and Al.

Inserting externally prepared films of various thicknesses into the beam path resulted in little data scatter for Al films only (Fig. 6). The oxide layers at the surfaces apparently arrested the film structure sufficiently, exposure to air and annealing having had little effect on the measured collector currents. Anneal of externally prepared Au and Ag films, however, could change collector currents by as much as a factor of 5; we found after stabilization by prolonged heating appreciable scatter of data points in current-versus-thickness plots. We attribute this fact to fluctuations in film thickness: Anneal favors the growth of the larger crystallites at the expense of the smaller ones, thus forming thin spots, which on account of exponential-thickness dependence strongly affect the apparent film transparency for electrons. Therefore, externally prepared films, 200 Å thick, of Au and Ag were used as substrates only, and film thickness was increased in the beam apparatus. The preparation conditions within the beam apparatus were identical to those employed for external film preparation. However, the evaporation geometry of the three filaments employed for *in situ* deposition required corrections of measured thicknesses for differences in distance and angle of incidence. With the assumption of a cosine distribution of evaporation intensity, excellent agreement was obtained in the data for films prepared from filaments at different positions.

The *in situ* mode of attenuation experiment for Au and Ag resulted in data showing negligible scatter (Fig. 4). Care had to be taken, however, to allow sufficient anneal in the case of Ag deposits. Deposition of Au at ambient substrate temperature or higher had little effect on the final result. However, Ag required deposition or annealing temperatures above 100°C for good reproducibility, especially when substrates of Au

[13] Westinghouse Electric Co.

[14] Basically, our attenuation data refer to mass penetrated by the electrons, which is directly measured by the oscillator crystal. Calibration of film thickness is correct if bulk density is independent of thickness. T. H. Hartman, Vacuum Sci. Technol. **2**, 241 (1965), found the density of Al films to decrease appreciably with the thickness below 500 Å, in contrast to A. R. Wolter, J. Appl. Phys. **36**, 2377 (1965), who found no density variation down to 200 Å (deposition rate 3–6 Å/sec at 10^{-6} Torr). Since no density measurements on Al films prepared under our production conditions are available, we have neglected this possible influence on our Al thickness calibration. No deviation from bulk density was observed by Hartman for Au and Ag films.

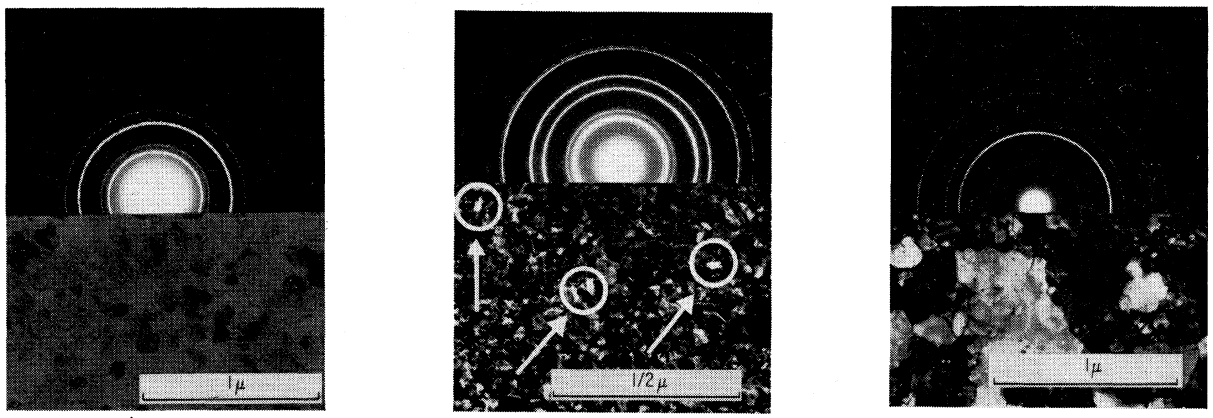

FIG. 7. Micrographs and diffraction patterns of: (a) Al film, (b) Ag film, and (c) Au film. Crystallite sizes, particularly for Au and Al, exceed the average film thickness many times. Note pinholes in the Ag film. The Al micrograph was taken slightly out of focus to make grain boundaries visible.

were used. Substrates of Au were preferred because of the difficulty of preparing pinhole-free Ag films in sufficient numbers. The use of Au substrates for Ag films had no apparent effect on the results. The only observable difference was a slight wrinkle due to stress differences that could not be removed by annealing. Films consisting of Au or Ag only generally appeared mirror flat after anneal.

Electron micrographs of films whose thickness was increased *in situ* were identical to those in Figs. 7(b) and 7(c). The Au films with Ag overlayers had a typical Ag texture superimposed on that of Au. That layers as thin as 20 Å increased the film thickness uniformly was deduced from the observation that attenuation lengths appeared to depend on neither layer nor substrate thickness. When total film thickness was increased by as much as a factor of 2, scatter of data points within one run was always negligible. Furthermore, clear energy dependence was apparent (Fig. 4) and tends to support the absence of "open areas." Bonding of condensing metal atoms on metal substrates appeared to be much stronger than observed on nonmetal substrates, thus effectively eliminating agglomeration.[15] While scatter of data points in Fig. 4, as in other runs, was negligible, the attenuation lengths measured in different runs did not agree within the same accuracy. The scatter variance between different runs is indicated by the error bars in Fig. 5.

That exponential-thickness dependence of collector current in itself does not prove film continuity was demonstrated on Al. The attempt to produce useful data with *in situ* deposits on (oxide-covered) Al support films failed. Attenuation fluctuated appreciably from run to run with considerable data scatter within one run. Micrographs clearly indicated island structure of the "*in situ*" layers, i.e., agglomeration was very effective in this case. The collector current, however, appeared to be exponentially dependent on thickness with $L\sim 56$ Å as compared with 40 Å measured on separately prepared films. The *in situ* data for Al were discarded.[16]

IV. TRANSPORT PROCESS

For the interpretation of our attenuation measurements, we considered the transport of a normally directed parallel beam of electrons through a metal film with nonscattering surfaces. Beam electrons are not collected when their *normal* energy component has decreased by more than 0.5 eV. Within the metal, the beam electrons interact with electrons, phonons, and imperfections (including impurities). The electron-electron collisions may be considered absorptive, since the associated energy loss is, on the average, large enough to prevent collection. From the results of Ritchie and Ashley[17] on the energy distribution of once-scattered electrons, we find that, after one collision, less than 2% of 5.5 eV primaries with an energy loss smaller than 0.5 eV remain. The proportion decreases with increase in energy. Electron-phonon collisions are considered to change momentum only since the associated energy loss (<0.03 eV) is negligible compared with the resolution. Because of the considerable probability of large momentum changes for electron-phonon processes at temperatures near or above the Debye temperature, the scattering distribution is generally considered isotropic (Sec. VI B). The average loss of normal momentum is correspondingly large. Only 2.5% of once isotropically scattered 5.5-eV electrons are collected. Electron-imperfection

[15] D. W. Pashley, Phil. Mag. 4, 324 (1959).

[16] The use of Au substrate films for *in situ* deposition of Al failed. Deposition at room temperature resulted in rupture at a Al thickness of less than 30 Å. Deposition under the best available vacuum conditions (pressure below 10^{-9} Torr during evaporation) onto Au films cooled to near 140°K resulted in attenuation lengths as small as 15 Å. The Al structure was nearly amorphous. Cu behaved similarly to Al.

[17] R. H. Ritchie and J. C. Ashley, J. Phys. Chem. Solids **26**, 1689 (1965).

scattering is essentially elastic but, as shown below, may be neglected in our results. Since $l_e \ll l_p$ in our experiments, multiple electron-phonon scattering resulting in an electron moving in the forward direction again is negligible. An electron-electron and electron-phonon collision, thus, effectively prevents collection. Consequently, the beam current decreases with $I_c \sim \exp(-D/L)$, where D is the film thickness and the ballistic-attenuation length is

$$L^{-1} = l_e^{-1} + l_p^{-1} \quad (1)$$

(l_e is the MFP for electron-electron collisions; l_p is the MFP for electron-phonon collisions).

Scattering at the surfaces, however, cannot be neglected. The influence of the boundaries on attenuation may be assessed as follows. We assume that the beam produces a source with a distribution somewhere between cosine and isotropic at the beam-side boundary for the following reasons: (a) The angular distribution of the beam is nonparallel because of the transverse velocity component, particularly if the normal velocity is near zero. (b) Because the crystallite surfaces are not necessarily in the surface plane, electrons are refracted over a range of angles. (c) A surface layer of foreign matter due to handling in air may contribute considerable scatter. (d) A film surface seems to be rough for slow electrons, since conduction electrons are usually more diffusely than specularly reflected at boundaries.[18] With a nearly cosine or isotropic source at the beam side of the film, the attenuation length near that boundary appears much shorter but approaches the ballistic length within a short distance (Appendix). Electrons traveling in non-normal direction die out more rapidly with depth as compared with those traveling in normal direction, resulting in a "self-focusing" effect.

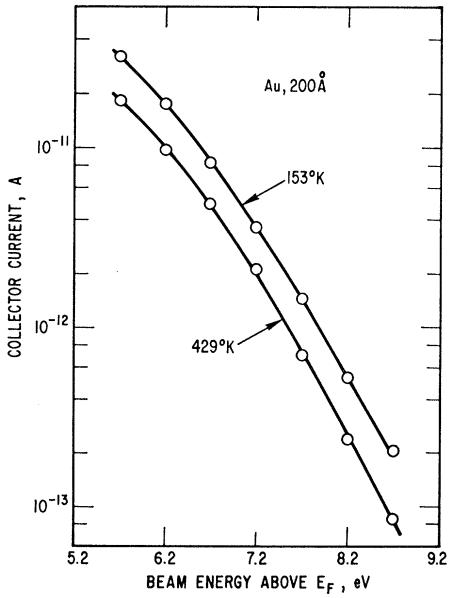

FIG. 8. Collector-current–versus–energy plots for two temperatures, indicating the approximate independence of both variables.

Considerable scatter also occurs at the second surface where a fraction of the electrons approaching in a nearly normal direction from the interior of the film emerge distributed over a range of angles. The electrons backscattered from the surface change the thickness dependence of the electron distribution from that of the interior, but because $l_e \ll l_p$, this occurs only within a shallow layer next to the surface. If the depth of this layer together with the depth of the nonexponential region near the source remains smaller than the film thickness, increase of the film thickness results in a collector current $I_c \sim \exp(-D/L)$ unaffected by the boundaries. The required minimum thickness appears to be of the order of 5 L, where the deviation of the observed attenuation from the ballistic attenuation is less than 5% (Appendix). Since no change of attenuation in film thickness was observed experimentally, we did not apply any correction for marginal film thicknesses.

The scatter on both surfaces is the reason for the observation that collector-current-versus-thickness plots did not extrapolate to incident current for zero thicknesses. Independent of energy and total thickness, for Au, a loss of about 0.02 occurred. Elastic scatter at the front surface can account for a factor of 0.36 (Appendix). Assuming a similar loss at the second surface would allow one to interpret a loss by nearly an order of magnitude as being caused by surface scatter. Since all films were handled in air and, thus, covered with surface layers, the actually measured loss of 0.02 does not appear unreasonable. In the case of Al, additional loss was caused by the oxide layers. Assuming surface losses of the same amount as observed in Au, we find that a factor of about 0.02 remains, which may be attributed to attenuation in the oxide. With an estimated total oxide thickness for both surfaces of near 35 Å,[19] the corresponding attenuation length is near 9 Å, in reasonable agreement with previous estimates.[20]

V. RESULTS

The attenuation lengths for Au and Ag in Fig. 5 and the value of $L \sim 40$ Å for Al are representative of the ballistic MFP (Sec. IV). To determine the contribution of electron-phonon collisions to this value, we studied the variation of attenuation with temperature. From Fig. 8, it is evident that, within the observed energy

[18] K. L. Chopra, L. C. Bobb, and M. H. Francome, J. Appl. Phys. **34**, 1699 (1963) and references quoted therein.

[19] J. E. Boggio and R. C. Plumb, J. Chem. Phys. **44**, 1081 (1966).

[20] R. E. Collins and L. W. Davies, Solid-State Electron. **7**, 445 (1964); E. D. Savoye and D. E. Anderson, J. Appl. Phys. **38**, 3245 (1967); F. L. Schuermeyer, C. R. Young, and J. M. Blasingame, *ibid.* **39**, 1791 (1968).

TABLE I. Electron-phonon MFP.[a]

	Au	Ag	Al	
$l_p(E_F+6\text{ eV})$ ballistic	280±30	425±30	250±50	10^{-10} m
$l_p(E_F)$ from conductivity data	~400[b]	520–580[c]	~400[d]	10^{-10} m
$l_p(E_F+1\text{ eV})$ ballistic[e]	406	570		10^{-10} m
ρ_B (295°K)	2.35	1.63	2.71	$10^{-8}\Omega$ m
$l_p(E_F+6\text{ eV})\rho_B$	6.6	7.0	6.8	$10^{-16}\Omega$ m^2
$l_r(E_F)$	2500	1200	>850	10^{-10} m
p	~0.7	~0.55	<1	
$l_e(E_F+6\text{ eV})$	42±7	38±4	50±5 (E_F+5 eV)	10^{-10} m

[a] Electron-phonon MFP values measured in this work are compared with published values valid at room temperature and at Fermi energy, where they are inversely related to the ideal bulk resistivity ρ_B. $l_p(E_F+1\text{ eV})$ refers to MFP values calculated on the basis of the free-electron gas model (Mott and Jones), which Crowell and Sze found in agreement with their ballistic data. l_r is the temperature-independent MFP contribution at the Fermi energy as deduced from conductivity measurements on our films. These l_r are considered lower limits for the energy- and temperature-independent MFP contribution at E_F+6 eV. p is the degree of specular Fermi electron reflection at the surfaces of films used to obtain l_r. l_e is the electron-electron MFP measured in this work.
[b] See Ref. 24; J. A. Johnson and N. M. Bashara, J. Appl. Phys. **38**, 2442 (1967); K. L. Chopra and L. C. Bobb, Acta Met. **12**, 807 (1964).
[c] See Ref. 25.
[d] A. F. Mayada, J. Appl. Phys. **39**, 4241 (1968).
[e] See Ref. 9.

range, energy and temperature variation appear independent of one another. Variables are, thus, separable, and the attenuation may be presented by

$$L^{-1}=l(E)^{-1}+l(T)^{-1}, \tag{2}$$

which is identical with Eq. (1) if we consider l_e to be the term determining the energy dependence and l_p as the term determining the temperature dependence. That this is a reasonable approximation may be seen from the following: (a) In metals, the electron-electron interaction process is temperature-independent because of the large average energy of the electrons ($E_F \gg kT$).[21] (b) Experimentally, the electron-phonon MFP at 6 eV was found to deviate only about 30% from its value at the Fermi level (Table I). Thus, l_p is only weakly energy-dependent if monotonous variation with energy is assumed. (c) An upper limit for contributions to Eq. (2) caused by imperfection and impurity scattering was obtained from bulk-resistivity measurements on our films and found to be negligible.

That $l(T)$ is representative of the MFP l_p for first-order electron-phonon interaction is concluded from the observed exponential dependence of collector current on temperature: $I_c \sim \exp(-T/T_0)$ (Fig. 9), where $1/T_0$ depends on film material and thickness (Fig. 10). Since also $I_c \sim \exp(-D/L)$, we have, with

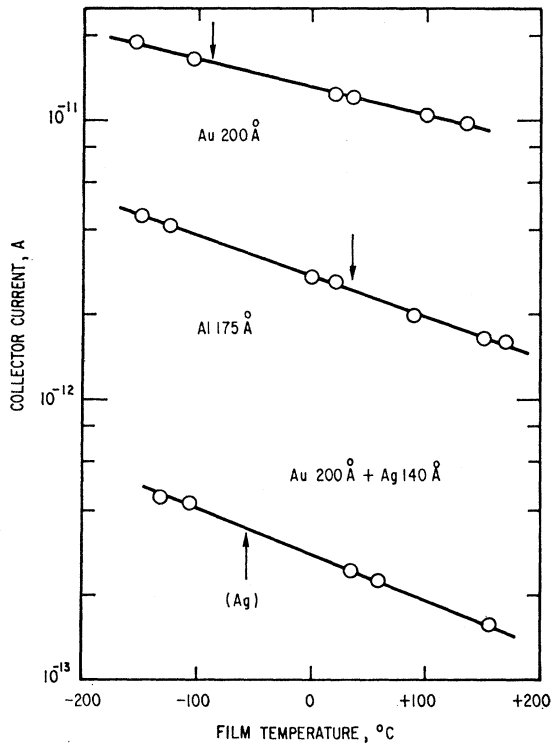

FIG. 9. Semilog plots of collector current versus temperature, indicating inverse dependence of electron-phonon MFP on temperature, i.e., the occurrence of primarily first-order processes. The arrows mark the Debye temperatures of the respective metals.

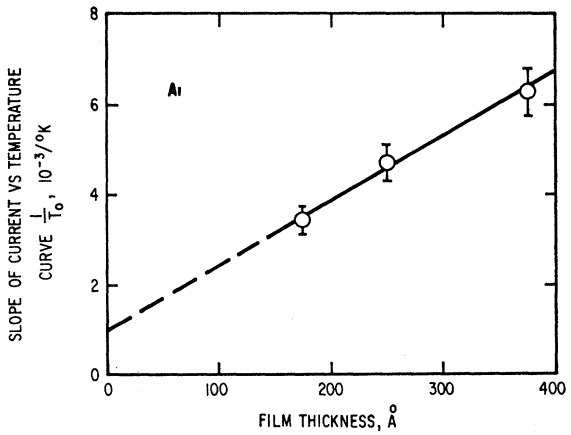

FIG. 10. Slope of the plots of Fig. 9 as a function of thickness for Al. From this, the electron-phonon interaction MFP is determined. That the line does not intercept the origin presumably reflects the contribution by the oxide layers.

[21] The effect of temperature on l_e through change in electron density by volume expansion is negligible.

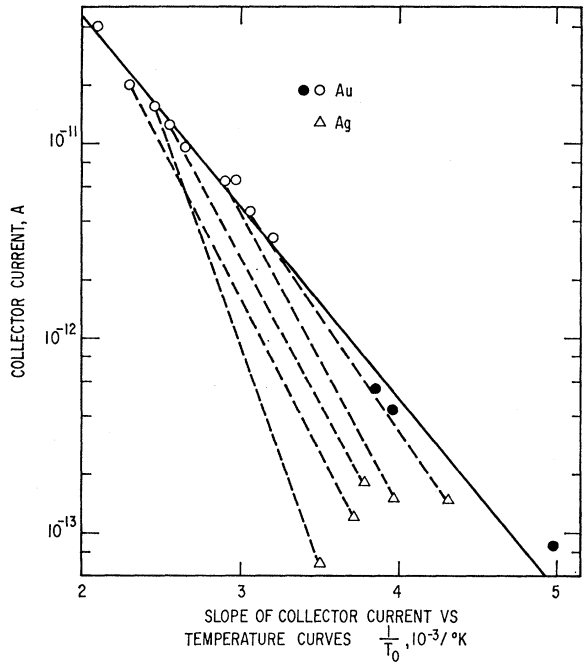

FIG. 11. Slope of the plots of Fig. 9 versus collector current for Au and Ag films. The collector current is a better measure of effective film thickness for these materials because of "thin spots." Circles refer to Au: the open ones to externally prepared films and the closed ones to films whose thickness was increased *in situ*. Triangles refer to Ag. Dashed lines indicate the change of current and slope for Ag deposited on Au supports. The slope of the lines in this figure was used to calculate the electron-phonon MFP with the help of Eq. (4).

Eq. (1), $I_c \sim \exp(-D/l_p)$. Identifying the temperature-dependent exponents $T/T_0 = D/l_p$, we find a temperature dependence of l_p, as expected for first-order processes. By measuring the change of $1/T_0$ with thickness (Fig. 10), we obtain the electron-phonon MFP

$$l_p = \frac{\Delta D}{\Delta 1/T_0} \frac{1}{T}. \tag{3}$$

Since for Au and Ag films the collector current appears to be a more reliable measure of effective thickness than the measured (average) thickness (Sec. III), we replace ΔD in Eq. (3) with $\Delta D = [\ln(I_2/I_1)]L$ and obtain l_p from the slope of $\ln I_c$-versus-$1/T_0$ plots (Fig. 11)

$$l_p = L \ln(I_2/I_1)(\Delta 1/T_0)^{-1} T^{-1}. \tag{4}$$

The measured electron-phonon MFP for all three metals are compared in Table I with published MFP values deduced from conductivity data and, thus, valid at the Fermi level.

An upper limit for possible "imperfection" contributions to the MFP, Eq. (2), was obtained from bulk-resistivity determinations made for annealed films while still settled on the nitrocellulose support. Bulk resistivity is inversely related to the MFP l_B at the Fermi level, which according to Mathiassen's rule is

$$1/l_B = [1/l(T)] + (1/l_r), \tag{5}$$

where $l(T)$ is the electron-phonon MFP and l_r is the MFP due to all other interactions. The electron-electron MFP at the Fermi level is large and neglected. For ideal bulk material at room temperature, $l_r \gg l(T) \sim l_B$; thus, by means of published values for $l(T)$, we can use deviations from ideal resistivity to calculate l_r. Both terms in Eq. (5) may generally vary with energy. l_r contains contributions by charged impurities and imperfections, which presumably contribute the strongest energy dependence for this term with the effect of increasing $l_r \sim E$.[22] Determination of l_r from conductivity data can, thus, be expected to give a lower limt for l_r that is valid at higher energies and applicable to scattering contributions other than electron-electron and electron-phonon interactions.

The bulk resistivity of our films was estimated from film-resistivity variations with thickness by means of an approximate formula based on the Fuchs-Sondheimer theory[23]

$$\rho = \rho_B[1 + 3l(1-p)/8D], \tag{6}$$

where D is the film thickness and p is the degree of specular reflectivity at the film surfaces. The formula is valid for $l/D > 1$, but accurate within 7% for $l/D > 0.1$. The ordinate intercept of ρ-versus-$1/D$ plots yields the bulk conductivity ρ_B, with which l_B can be calculated and l_r can be obtained by use of Eq. (5). The latter values are listed in Table I together with the degree of specular reflectivity derived from the slope of the plots. As a further check for Au, the temperature variation of resistivity was measured. Our Au film results were in good agreement with those published recently by Broquet and Nguyen Van.[24] The Ag films show specularities larger than reported by Chopra and Randlett,[25] who measured $p \sim 0$ for thickness-versus-MFP ratios investigated here. The Al-film resistivity appeared to change little with thickness, thus $p \sim 1$. Since, according to Eq. (6), ρ_B increases with increase of p, $p \sim 1$ results in a lower limit for l_r but is still applicable for the estimate.[26]

[22] J. M. Ziman, *Electrons and Phonons* (Oxford University Press, London, 1960), p. 223.

[23] E. H. Sondheimer, *Advances in Physics* (Taylor and Fravers, Ltd., London, 1952), Vol. 1, p. 1.

[24] P. Broquet and V. Nguyen Van, Surface Sci. **6**, 98 (1967).

[25] K. L. Chopra and M. R. Randlett, J. Appl. Phys. **38**, 3144 (1967).

[26] A number of recent papers [Ref. 25; J. A. Johnson and N. M. Bashara, J. Appl. Phys. **38**, 2442 (1967); K. L. Chopra and L. C. Bobb, Acta Met. **12**, 807 (1964); A. F. Mayada, J. Appl. Phys. **39**, 4241 (1968); K. L. Chopra, Phys. Rev. **155**, 660 (1967); Y. Namba, J. Appl. Phys. **39**, 6117 (1968)] on size effect in thin metal films have shown that resistivity changes with thickness for very thin films are usually more drastic than expected on the basis of the Fuchs-Sondheimer theory. The simple approach taken here to estimate l_r can, thus, lead to erroneous results. We believe, however, that on account of the smallness of l_e as well as l_p, compared with usually observed l_r our estimate of a lower limit for l_r is adequate.

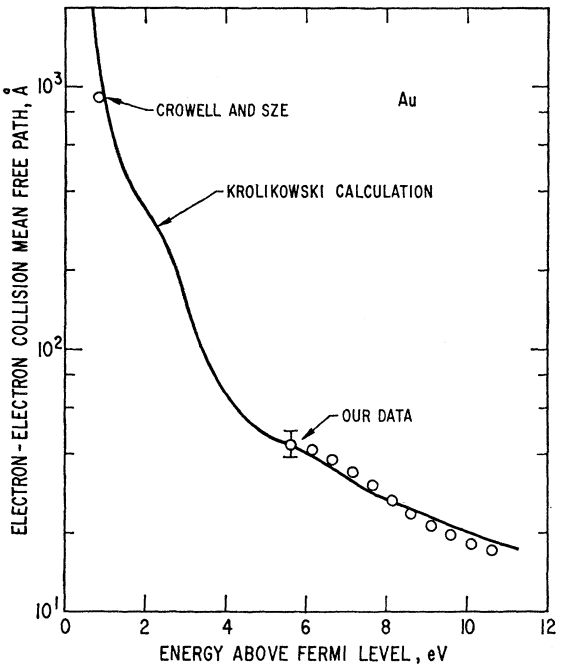

FIG. 12. Experimental MFP values for electron-electron interaction in Au. Data from this work and by Crowell and Sze (Ref. 3) are shown. The curve is calculated, except for the arbitrary factor, by Krolikowski (Ref. 4) using the optical density-of-state distribution displayed in Fig. 14 and assuming nonconservation of momentum, constancy of the matrix element, and the applicability of the one-electron model.

The limits of the imperfection MFP obtained by this method generally account for less than a 10% correction to our l_e MFP results. Because of the smallness of this contribution and the conceivable objection that the conduction MFP valid for electron transport in the plane of the film, which is hindered by many grain boundaries, might not be applicable to transport in the direction of the film normal, we have neglected imperfection contributions altogether. The conductivity data, however, might serve as an indicator of the quality of the films used in our experiments.

Determination of the electron-electron collision MFP requires that the measured attenuation lengths need to be corrected for the electron-phonon contribution only.[27] The resulting l_e values for 6 eV are listed in Table I. Since we could not observe any variation of l_p with energy within our experimental accuracy, we consider the electron-phonon MFP to be constant between 5 and 10 eV and find the energy dependence of the electron-electron MFP as shown for Au in Fig. 12 and for Ag in Fig. 13. The results are compared with other experimental data and theoretical predictions in Sec. VI.

[27] We neglect scattering by diffraction since no quantitative information is available. Diffraction at energies here under consideration has been demonstrated by J. G. Simmons *et al.*, Phys. Rev. Letters **17**, 675 (1966).

VI. DISCUSSION

A. Electron-Electron Process

A self-consistent calculation of electron-electron interaction MFP in an electron gas has been given by Quinn and Ferrell.[28] The imaginary part of the self-energy of the excited quasiparticles, which is proportional to the transition rate (or damping), is obtained by integrating $\mathrm{Im}\epsilon^{-1}$ over the available momentum space as follows:

$$\frac{1}{\tau}=2E_I=\frac{2e^2}{\pi}\int\frac{dk^3}{4\pi k^2}\,\mathrm{Im}\epsilon^{-1}(\Delta k,\Delta E), \qquad (7)$$

where $\epsilon(\Delta k,\Delta E)$ is the dielectric function depending on momentum and energy change of the excited quasiparticles. For the concept of lifetime τ to remain meaningful, Eq. (7) is restricted to values of the imaginary part of the self-energy that are small compared with the real part of the energy. Using Lindhard's expression[29] of the dielectric function for a free-electron gas in the high-density limit, Quinn[6] obtains the MFP

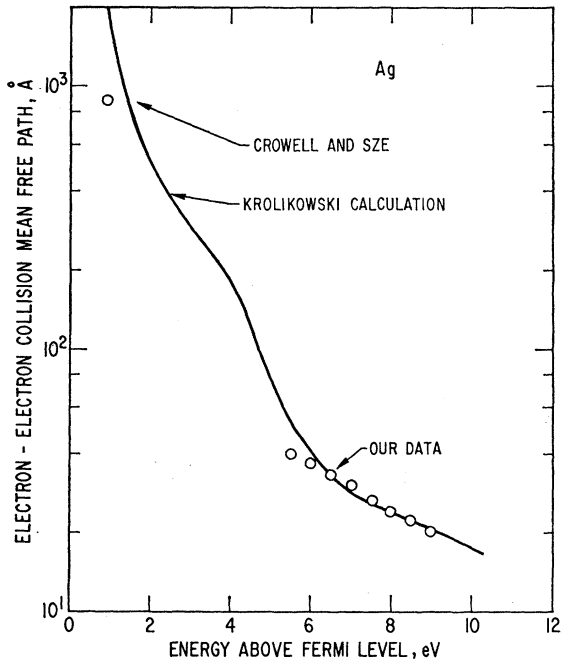

FIG. 13. Experimental MFP values for electron-electron interaction in Ag. Data from this work and by Crowell and Sze (Ref. 3) are shown. The curve is calculated, except for the arbitrary factor, by Krolikowski (Ref. 4) using the optical density-of-state distribution displayed in Fig. 14 and assuming nonconservation of momentum, constancy of the matrix element, and the applicability of the one-electron model. Note that our experimental points do not indicate the sharp rise with decrease of energy, as expected on the basis of the calculated curve.

[28] J. J. Quinn and R. A. Ferrell, Phys. Rev. **112**, 812 (1958).
[29] J. Lindhard, Kgl. Danske Videnskab. Selskab, Mat.-Fys. Medd. **28**, No. 8 (1954).

from Eq. (7) and $l_e=\tau\bar{v}$. The result is

$$l_e=\frac{14.7(E_F\beta)^{3/2}E}{(m^*)^{1/2}\{\tan^{-1}\beta^{-1/2}+[\beta^{1/2}/(1+\beta)]\}}(E-E_F)^{-2}, \quad (8)$$

where β is $(4/9\pi)^{1/3}(r_s/\pi)$ and r_s is the radius of the volume element per electron measured in Bohr radii.

The dielectric approach of Eq. (7) is strictly correct for $r_s\leq 1$ only, but calculations of DuBois[30] indicate that this approach is reasonably good even for $1<r_s<2$. In real metals, it is found that $r_s\gtrsim 2$ [r_s(Al)$\sim$2.1; r_s(Au)$\sim$3.2]. Al with 3 electrons per atom in the conduction band (the next tighter levels of the L shell are about 70 eV below the conduction band) is generally considered a good representative of a metal with a nearly free-electron system at a density still reasonably within the range of the Lindhard approximation of Eq. (8). Furthermore, the excitation energy used in our experiment is sufficiently close to the Fermi level, and the imaginary part of the self-energy is small enough compared with the real part so that Eq. (8) is applicable. We find, for Al, $l_e\sim 57$ Å at 5 eV. The theoretical estimate compares favorably with our experimental result of $l_e\sim 50$ Å.

The theoretical prediction may be improved by consideration of the deviations of the dielectric function from Lindhard's high-density limit at real metal densities, which must be expected because of exchange and correlation effects.[31] Improved calculations of the dielectric functions have been the subject of considerable recent activity.[7,17,32] The most advanced calculation based on a self-consistent field approach and still practical enough to allow the evaluation of the imaginary part of the self-energy appears to be the work by Kleinman.[7] According to this work, exchange apparently hinders the "degrees of freedom" of the screening electrons of parallel spin through the exclusion principle and, thus, reduces the magnitude of the dielectric function as compared with the high-density limit. Referring to Eq. (7), a larger transition rate or, correspondingly, a smaller MFP is then expected. Quantitative exchange corrections to Lindhard's dielectric function have to await numerical evaluation of Kleinman's theory,[33] but the correction to the self-energy is not expected to be appreciably in excess of 10–20%. A correction of this size would remove the remaining discrepancy between theory and experiment.

Unfortunately, we were unable to measure the variation of L with energy for Al and, thus, could not check the energy dependence predicted by Eq. (8). We instead compared our data with those of other investigators for other energies obtained by different experimental methods.

Huber *et al.*[8] made comparable measurements of attenuation in Al. These authors determined the attenuation length by measuring the current transfer through triode *M-I-M-I-M* sandwich structures as a function of thickness of the central metal film (*M* is the aluminum, *I* is the aluminum oxide). The energy was determined by the "emitter bias" and the "collector" barrier height and was in the range between 2 and 3 eV. Essentially different from previous tunnel experiments was the relatively low bias across the very thin "emitter" insulator ($\sim$40 Å); thus, tunneling into the conduction band of the insulator where considerable electron losses occur was avoided. The authors were able to provide evidence that their measured L was essentially ballistic. Hence, their experimental technique is conceptually quite similar to ours, and a comparison appears justified. They found $L\sim 150$ Å at 77°K. From this, we may roughly estimate l_e near 2.5 eV as follows: If we assume l_p at 2.5 eV and room temperature to be half-way between $l_p=400$ Å at the Fermi level and $l_p\sim 250$ Å at 5 eV (Table I) and consider an approximate inverse temperature dependence, we find $l_p\sim 1200$ Å at 2.5 eV and 77°K. The imperfection MFP for the films used by Huber *et al.* is expected to be of the same order as observed in our films. Assuming $l_r\sim 850$ Å, we find $l_e\sim 200$ Å, which is to be considered an upper limit in the case where l_r is actually larger. Quinn's theory, Eq. (7), predicts $l_e\sim 180$ Å. The estimated l_e for 2.5 eV is, thus, as close to theoretical predictions as found at 5 eV. The measurements by Huber *et al.* may, therefore, be considered consistent with ours.

The only other MFP determination for Al is, to the author's knowledge, that by Stuart and Wooten.[34] They found $l_e\sim 510$ Å and $l_p\sim 130$ Å, or $L\sim 105$ Å, valid at 9 eV. These values, particularly l_e, are in considerable disagreement with our data. However, their data are not based on attenuation measurements but were obtained from photoelectron energy distributions and yield measurements that were fitted with the results of Monte Carlo calculations. In view of the difficulties of measuring all pertinent parameters accurately in photoemission experiments, the disagreement with our data is perhaps not too surprising.

Turning next to Au and Ag, the MFP dependence on energy could be obtained for both materials between 5 and 10 eV. Furthermore, our data can be directly compared with the experimental data at about 1 eV obtained by Crowell and Sze.[3] Unfortunately, no precise theory is available for these materials, which are characterized by the presence of the more tightly bound *d*-band electrons, overlapping into the conduction band. In what follows, we compare the experimental data with the estimates that are presently available.

[30] D. F. DuBois, Ann. Phys. (N. Y.) **7**, 174 (1959).

[31] S. L. Adler [Phys. Rev. **130**, 1654 (1963); **141**, 814 (1966)] has shown that solid-state effects, i.e., umklapp processes and local-field corrections contribute negligibly to energy-loss rate.

[32] L. Kleinman, Phys. Rev. **160**, 585 (1967); K. S. Singwi, M. P. Tosi, and R. H. Land, *ibid.* **176**, 589 (1968); S. Strässler, *ibid.* **180**, 517 (1969); K. L. Kliewer and R. Fuchs, *ibid.* **181**, 552 (1969).

[33] F. Vernon and L. Kleinman (unpublished).

[34] R. N. Stuart and F. Wooten, Phys. Rev. **156**, 364 (1967).

Quinn's theory has been used to evaluate the electron-electron MFP in Au and Ag at energies near 1 eV, where interaction with the lower d-band electrons does not occur yet. However, the polarizability of the d-band electrons and their screening effect had to be taken into account.[35] Considering exchange and d-band screening, Crowell and Sze,[3] using Eq. (8), estimate a MFP for both materials of roughly 1000 Å at 1 eV, which they find to be in reasonable agreement with their experimental results. The data were obtained from ballistic-path determinations in metal films sandwiched between semiconductor contacts. The barrier heights determined emitter and collector energy. Measurement of the temperature dependence allowed the elimination of the contribution by electron-phonon interactions. The experimental approach of these authors is believed to give results more accurate than was possible in earlier experiments utilizing the photoelectric effect. Crowell and Sze's data points are indicated in Figs. 12 and 13, respectively.

At the energies used in this work, interaction of the excited electron with the deeper d band is energetically possible, and Quinn's theory derived for a free-electron gas in the high-density limit is not applicable. Instead, we use the results of a semiempirical approach employed by Krolikowski and Spicer[4] to obtain the energy dependence of the electron-electron MFP for the range between 1 and 10 eV for both Au and Ag. The authors assume the probability for transition of an excited state to be proportional to the product of the following factors[36]: (1) the number of valence electrons per energy interval with which the excited electron can interact, (2) the density of the final states of the incoming electron, and (3) the density of the final states of the valence electron. The total transition probability for the excited state is obtained by integrating over all energetically accessible states,

$$\frac{1}{\tau(E)} = P(E) \sim \int_{E_F}^{2E_F-E} d(E_V) \int_{E_F-E_V}^{E-E_F} d\Delta E \times N_V(E_V) N_C(E-\Delta E) N_C(E_V+\Delta E), \quad (9)$$

where N_V and N_C are the density of occupied and unoccupied states, respectively; E and $E-\Delta E$ refer to the initial and final energy of the incoming electron and E_V and $E_V+\Delta E$ to that of the valence electron, respectively. The MFP is deduced with $l(E) \sim \tau(E)\langle v\rangle$, $\langle v\rangle$ being the average electron velocity.

An essential assumption on which this approach depends is that k conservation is not important in the transition process.[37] The assumption, thus, concurs with the result of energy-distribution measurements on photoexcited electrons for a certain class of materials. For these materials, which include Au and Ag, Spicer *et al.* were led to conclude that the energy-distribution curves could be understood and used for the deduction of density-of-states distributions if k was assumed not to be an important quantum number. In the light of this experience, Krolikowski and Spicer's assumption leading to Eq. (9) appears to be reasonable if one expects the nature of the energy source for valence-electron excitation to be of minor importance, i.e., if the finite contributions of k by the exciting electron (in contrast to $k=0$ for photons) are of no consequence. In fact, agreeing with the above, Kane[38] found from calculations of the inelastic electron scattering by pair production in silicon that results were very similar, regardless of momentum conservation.[39] Consequently, the use of the density of states in Eq. (9) obtained from energy-distribution curves of photoemitted electrons can be expected to give reasonable predictions of the relative change of MFP with energy.

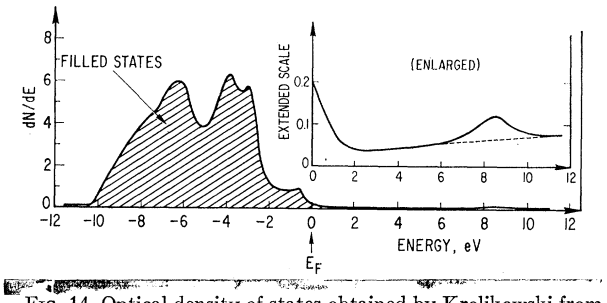

FIG. 14. Optical density of states obtained by Krolikowski from photoelectron energy distributions on Au. Nonconservation of momentum and independence of matrix element on energy was assumed.

Using the density of states obtained by photoemission experiments (shown for Au in Fig. 14), Krolikowski and Spicer computed, with Eq. (9), the energy dependence of MFP for Au and Ag. The resulting curves adjusted to our experimental values are drawn in Figs. 12 and 13, respectively. It should be mentioned that the method for obtaining the optical density of states does not give information for energies between the Fermi level and the work function of the material (about 4.9 eV for Au and 1.6 eV for Ag whose work function was lowered by a cesium overlayer) and that, therefore, values for these energy ranges were extrapolated. The value at the Fermi level was adjusted for specific-heat values in accordance with published values. The integration process of Eq. (9), however, tends to mask any possible

[35] J. J. Quinn, Appl. Phys. Letters **2**, 167 (1963).
[36] C. N. Berglund and W. E. Spicer, Phys. Rev. **136**, A1030 (1964).
[37] Other assumptions are the occurrence of single-electron collisions only with a matrix element independent of energy.
[38] E. O. Kane, Phys. Rev. **159**, 624 (1967).
[39] W. E. Spicer [Phys. Rev. **154**, 385 (1967)] gives possible reasons for k not being an important quantum number that appear to be related (in the case of the noble metals) to rapid relaxation effects through the surrounding electrons on the localized hole left in the d band during the excitation process. Since this many-body effect may significantly contribute in the optical excitation process, the density-of-state distributions deduced from energy distribution curves of photoexcited electrons are labeled "optical density of states," in contrast to the possibly different density of states appropriate to the ground state.

(weak) structure that might actually exist in the extrapolated ranges.

As apparent from Figs. 12 and 13, Krolikowski and Spicer's MFP-versus-energy curve reproduces present experimental findings quite well in the case of Au, less satisfactorily in the case of Ag. For Au, the following is observed: (1) The slope of our experimental values and that of the computed curve agree; (2) the experimental data reproduce quite nicely the slight depression of the MFP near 7 eV, which is caused by the peak at -6 eV in the optical density-of-states distribution (Fig. 14); and (3) both our data and that of Crowell and Sze at 1-eV energy is connected by the curve.

Agreement at 1 eV is less satisfactory for the case of Ag. For this material, the slope of the MFP curve approximately reproduces that of our experimental data. However, the experiment fails to indicate the steep rise of the calculated MFP for energies below about 6.5 eV. This deviation is perhaps suggestive of a contribution of collective response of the electron system to damping of the excited single-electron state, which is not accounted for when applying the density-of-states concept. Ag has a volume plasma resonance near 3.75 eV and a surface plasma resonance near 3.6 eV. While Berglund and Spicer[40] did not observe any indications of plasma effects in their photoemission experiments that were carried out below 11 eV, surface plasma interaction at these excitation energies has recently been demonstrated.[41] The deviation near 5 eV, which we believe to be outside experimental error, therefore, might be caused by a collective response unless the reason is the uncertainty of the exact position and sharpness of the d-band edge in the optical density-of-states distribution.

In concluding this subsection, we observe that the experimentally determined MFP's for electron-electron interaction appear to agree reasonably well with theoretical expectations for Al and, furthermore, seem to support the MFP-versus-energy dependence on the basis of optical density of states obtained from photoemission experiments for Au and Ag, i.e., the single-electron model is a good approximation at energies here under consideration. The degree to which many-body effects contribute to electron excitation in the vicinity of the Fermi level through screening by lower-lying bands or through plasma damping at energies in excess of the resonance can only be assessed after more experimental information is available.

B. Electron-Phonon Process

In this subsection, we emphasize the observation that the measured electron-phonon MFP above the 5-eV energy level appears to be appreciably smaller than for energies near the Fermi level. We have listed published electron-phonon MFP at the Fermi level found from conductivity data (Table I). Since conductivity measures the transport MFP $[\lambda(1-\langle\cos\mu\rangle_{\rm av})^{-1}$, where λ is the collision MFP, and $\langle\cos\mu\rangle_{\rm av}$ is the average cosine of the deflection angle], any deviation from isotropy of the scattering process ($\langle\cos\mu\rangle_{\rm av}\neq 0$) would lead to an increase of the transport over the collision MFP, the latter being determined in our experiments. Crowell and Sze,[42] however, measured the electron-phonon collision MFP when they determined the temperature-dependent part of attenuation in thin films between closely spaced semiconductor contacts. For Au, they found $l_p\sim 400$ Å at 1 eV in agreement with the conductivity MFP. (If any variation of l_p with energy within 1 eV of the Fermi level is negligible, this agreement might be considered an experimental confirmation of the theoretically ascertained isotropy[43] of the electron-phonon scattering process in noble metals near or above the Debye temperature.) Furthermore, when using the conduction MFP in Ag, $l_p\sim 570$ Å, the same authors[3] deduced from attenuation measurements on Ag near 1 eV an electron-electron collision MFP $l_e\sim 1200$ Å, a value nearly equal to that of Au (Figs. 12 and 13), which appears quite reasonable on account of the similarity of the conduction bands in the vicinity of the Fermi level in both materials. We may then conclude that electron-phonon MFP applicable to ballistic measurements at 1 eV for Au and Ag are in reasonable agreement with those determined from thin-film conductivity data. In contrast, l_p above 5 eV is only about two-thirds of l_p near E_F for all three materials investigated.

We were unable to resolve a decrease of l_p with increasing E within the investigated range of 5–7 eV. However, if we assume that the electron-phonon MFP varies inversely with energy, the expected variation is too small to be resolvable with our experimental accuracy. The lack of discernible variation, is, thus, compatible with a "smooth" decrease of l_p with increasing energy.

It could be argued that the observed electron-phonon MFP is smaller than bulk value because of considerable surface area at film and grain boundaries. Near surfaces, the ion amplitudes are larger because of reduced binding, resulting in stronger electron scattering. We can obtain an estimate of the effect on l_p by using the results of Jones *et al.*,[44] who determined the ion amplitude at Ag surfaces from Debye-Waller factors in low-energy electron diffraction (LEED) experiments. These authors found the average squared deviation from equilibrium position to be about twice that for the

[40] C. N. Berglund and W. E. Spicer, Phys. Rev. **136**, A1044 (1964).

[41] H. Mayer and J. Hölzl, Phys. Status Solidi **18**, 779 (1966); T. A. Callcot and A. U. MacRae, Phys. Rev. **178**, 966 (1969); A. U. MacRae, K. Muller, J. J. Lander, J. Morrison, and J. C. Phillips, Phys. Rev. Letters **22**, 1048 (1969).

[42] C. R. Crowell and S. M. Sze, Phys. Rev. Letters **15**, 659 (1965).

[43] P. L. Taylor, Proc. Roy. Soc. (London) **A275**, 209 (1963).

[44] E. R. Jones, J. T. McKinney, and M. B. Webb, Phys. Rev. **151**, 476 (1966).

bulk with the "excess" decreasing with e^{-n} towards the interior, n being the number of atomic layers. Since l_p is inversely proportional to the average squared amplitude, one can easily determine how many surfaces are required for a number of atomic layers in order to observe a certain decrease in l_p. Considering only surfaces perpendicular to the electron path, it turns out that, at most, three atomic layers per surface are required for a decrease of l_p by a factor of about 0.6. Accordingly, our films had to consist of grains about 25 Å average size in order to make a bulk MFP value, unchanged from that at the Fermi energy, appear as short as observed in our experiments. For larger grains, the surface effect rapidly diminishes (10% decrease in l_p for 80 Å grain diameter), although oblique crossing of surfaces of electron trajectories somewhat increases the effect. According to our film micrographs (Fig. 7), the required average small grain size could at best have existed in the Ag films, but certainly not for Au or Al. However, the decrease of l_p compared to bulk values at Fermi energy is observed for all three materials in the same proportion. We are led to conclude that our measured l_p are essentially undisturbed by surface effects and are, thus, representative of bulk values. While changes of l_p due to the proximity of the film surfaces cannot be completely ruled out, we believe the decrease of l_p with increase of E to be a bulk effect.

It is beyond the scope of this work to discuss all possible reasons for an energy dependence of the electron-phonon MFP. It might suffice to indicate which factors might cause the variation with energy. Since we can write $l_p \sim \langle v \rangle (M^2 \zeta)^{-1}$, with M as the matrix element, $\langle v \rangle$ as the group velocity, and ζ as the electron density of states, one would expect, for a free-electron gas with $\langle v \rangle$ and ζ both proportional to $E^{1/2}$, the electron-phonon MFP to vary very little in the case where the matrix element is at most weakly energy-dependent. The experiment indicates that in the investigated materials either M varies considerably with energy or the energy dependence of $\langle v \rangle$ and ζ differ appreciably. A theory clearly indicating the observed energy dependence does not exist presently.

VII. CONCLUSION

The feasibility of beam-attenuation measurements on thin metal films at energies in the electron-volt range has been demonstrated. Electron-electron interaction as well as electron-phonon interaction MFP can be determined and their variation with energy studied. The influence of film structure is appreciable but can be minimized if the crystallite size in the film plane exceeds the average film thickness. The method used in this work appears to be extendable to a wider range of energies and to other metals. Application of barrier-lowering overlayers to the film surfaces should permit measurements at energies closer to the Fermi level (i.e., ~1.5 eV for cesium on Ag). By optimization of beam current and application of better low-current detection techniques, the energy range can be increased to larger values. Increased detection sensitivity would also have the advantage of permitting an experimentally useful increase in film thicknesses. On the lower end, film thickness is limited by the need to avoid pinholes; on the upper end, by the minimum detectable current. Metals that require larger minimum thicknesses or attenuate stronger could then be investigated by the same method. A further requirement for attenuation measurements with attenuation lengths in order of a few tens of angstroms is the avoidance of excessive agglomeration during deposition, which prevents the formation of reasonable uniform thickness increments. Metal supports appear to provide sufficient bonding for the condensing atoms to effectively eliminate agglomeration. However, alloying and stress effects appear to limit the use of support films of a metal (Au in this work) different from that formed by *in situ* deposition. The possibilities of other support films, i.e., carbon films, have not been explored. It seems feasible to extend the measurements to other sufficiently conducting materials without resort to complicating pluse techniques, which, because of charging effects, would be required for insulating materials. The accumulation of consistent experimental data on electron interaction for a variety of real interacting electron systems should aid the development of self-consistent many-body theories, which is of consderable current interest.

ACKNOWLEDGMENTS

The author wishes to thank Dr. J. Munushian and Dr. F. Vernon for stimulating discussions and constant encouragement. Illuminating conversations with Professor L. Kleinman on the implications of his theory are appreciated. Thanks are due Professor W. E. Spicer and Dr. W. F. Krolikowski for making their data available prior to publication and Professor Spicer for critical comments on the manuscript. The assistance by H. Luckey during the experiments is appreciated.

APPENDIX

Consider a beam of electrons impinging perpendicularly on a semi-infinite metal slab. At the boundary, the electron trajectories are deflected through a range of angles. We measure that portion of electrons actually entering the metal, with a maximum deflection angle of $\frac{1}{2}\pi$, i.e., the current crossing the surface plane. In the interior, electrons are absorbed along their respective paths with an attenuation length L. We ask for the decrease of the current component I_n in the normal direction as a function of depth D. If we denote the scattering distribution at the surface with $f(\theta)$, we find

$$I_n(D) = I_0 \frac{1}{N} \int_0^{\pi/2} d\theta \, f(\theta) \cos\theta \sin\theta \, e^{-D/(\cos\theta)L}, \quad \text{(A1)}$$

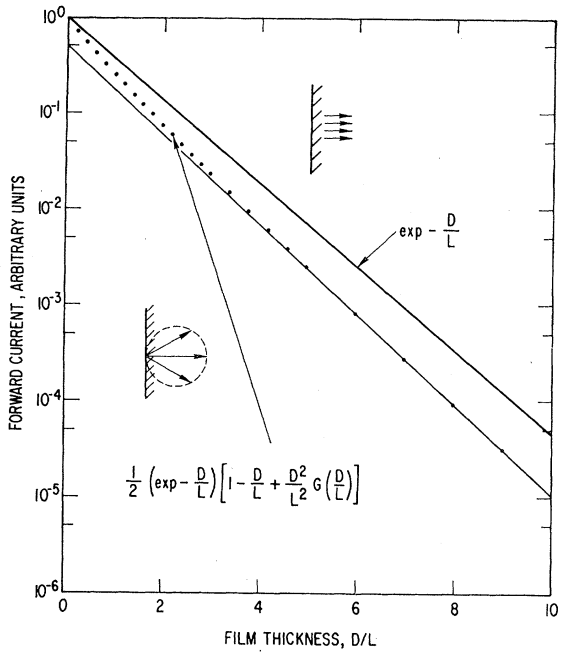

FIG. 15. Forward current in an absorptive semi-infinite medium as a function of depth for unidirectional and source with a cosine distribution (dotted line) at boundary. In both cases, the same number of particles enter the medium. At depths of more than four attenuation lengths, the decay for a source with a cosine distribution is practically exponential with an attenuation length deviating by less than 5% from that of the unidirectional case. By extrapolating the curve for $D \geq 6L$ to zero thickness (lower solid line), one finds a "loss" of electrons by a factor of 0.48 as compared with the unidirectional case.

where I_0 is the total current entering the metal, θ is the deflection angle, and N is a normalizing factor depending on $f(\theta)$. The solution for $f(\theta)=1$ (isotropic distribution) is

$$I_n(D)=I_0\left[1-\frac{D}{L}+\left(\frac{D}{L}\right)^2 G\left(\frac{D}{L}\right)\right]\exp\left(-\frac{D}{L}\right), \quad \text{(A2)}$$

and for $f(\theta)=\cos\theta$,

$$I_n(D)=I_0\left\{1-\frac{D}{2L}\left[1-\frac{D}{L}+\left(\frac{D}{L}\right)^2 G\left(\frac{D}{L}\right)\right]\right\} \times\exp\left(-\frac{D}{L}\right), \quad \text{(A3)}$$

where[45]

$$G\left(\frac{D}{L}=\zeta\right)=\frac{1}{\zeta+}\,\frac{1}{1+}\,\frac{1}{\zeta+}\,\frac{2}{1+}\,\frac{2}{\zeta+}\,\frac{3}{1+}\,\frac{3}{\zeta+}\cdots$$

is a function related to the incomplete γ function. Equation (A3) is plotted by dots in Fig. 15. It is obvious that the observed attenuation length (in normal direction), as well as the ordinate intercept obtained by straight-line extrapolation to zero thickness, depends on the depth at which measured. From numerical evaluation, we find that for depths $D \geq 4L$ the deviation of the measured attenuation length from the actual one is smaller than or at most equal to 5%, depending on $f(\theta)$. Corrections to measured L values for proximity to the entrance surface have, thus, been neglected. The ordinate intercept of the tangent to the curve represented by Eq. (A2) or (A3) for $D \geq 6L$ was found to be ≤ 0.36 for isotropic distribution and ≤ 0.48 for cosine distribution. These figures represent the "apparent loss" due to elastic scattering at the entrance surface.

An estimate of the apparent loss at the second or exit surface in our experiments depends on what fraction of the current approaches the surface within the escape cone. For electrons 6 eV above the Fermi level in Au with a work function of 5.2 eV and a Fermi energy of 5.5 eV, the escape-cone angle is about 15°. With $f(\theta)=\cos\theta$ at $D=0$, the angular distribution of current at $D \sim 6L$ has a most probable direction of $\theta \approx 20°$ with 90% of all electrons being within $\theta \approx 35°$, as determined from the integrand of Eq. (A1). In the case where the surface is perfectly flat, our estimate of the fraction of current able to escape (or the loss factor) is 0.3.[46] Deviation of crystallite surface directions from the normal of the film plane may reduce the loss factor somewhat.

Combining both loss factors, we find that we can, at best, explain about an order of magnitude of current loss due to (elastic) scattering at both surfaces. In contrast, the experimentally determined loss factor is close to 0.02, i.e., we have to assume additional loss mechanisms at the surface that remove electrons from the beam. In view of the fact that all our substrate films were handled in air and resulted in surface coverage of an unknown nature (presumably mostly water), the observed larger surface loss does not appear unreasonable.

[45] *Handbook of Mathematical Functions*, edited by M. Abramowitz and I. A. Stegun (U. S. Department of Commerce, National Bureau of Standards, Washington, D. C., 1964), Appl. Math. Ser. 55.

[46] This value increases with increase in thickness; however, the effect is negligible for the range of thicknesses here under investigation.

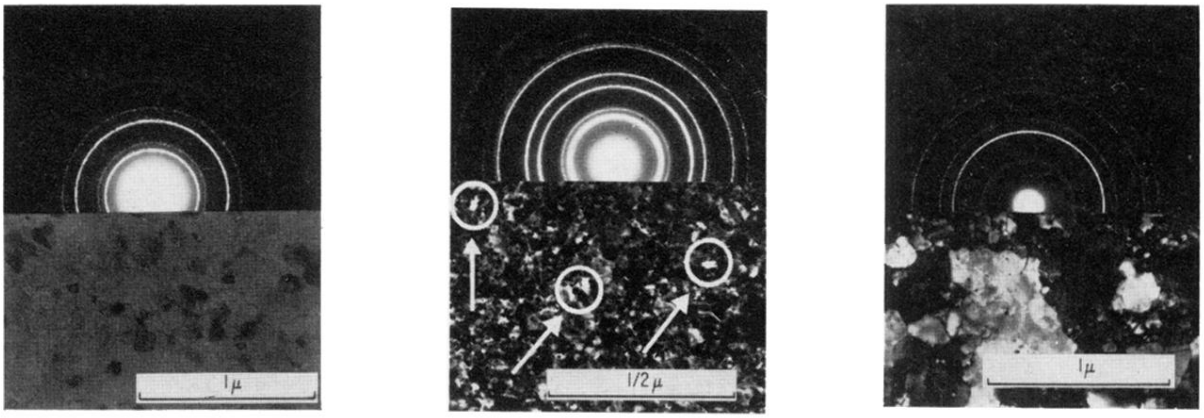

FIG. 7. Micrographs and diffraction patterns of: (a) Al film, (b) Ag film, and (c) Au film. Crystallite sizes, particularly for Au and Al, exceed the average film thickness many times. Note pinholes in the Ag film. The Al micrograph was taken slightly out of focus to make grain boundaries visible.